Journal of Applied Polymer Science

Synthesis and Characterization of PLA Nanocomposites Containing Nanosilica Modified with Different Organosilanes II: Effect of the Organosilanes on the Properties of Nanocomposites: Thermal Characterization

Luca Basilissi, Giuseppe Di Silvestro, Hermes Farina, Marco Aldo Ortenzi
Dipartimento di Chimica, Università degli Studi di Milano, Via Venezian 21, I-20133 Milano, Italy
Correspondence to: L. Basilissi (E-mail: luca.basilissi@unimi.it)

ABSTRACT: Thermal behavior of polylactic acid (PLA)/nanosilica nanocomposites prepared via bulk ring opening polymerization from lactide was investigated by differential scanning calorimetry and thermogravimetric analysis (TGA). Both unmodified nanosilica and modified by surface treatments with different amounts of two distinct silanes were used. Samples containing pure silica show enhanced crystallization processes; with silane-modified silica this effect is magnified, especially in the case of materials with high loadings of epoxy silane. Nonisothermal crystallization temperatures become higher and isothermal crystallization kinetics show a marked increase of Kinetic constant (K_c). TGA analyses show that, when pure nanosilica is present, nanocomposites have a thermal stability far greater than the one of standard PLA, starting their degradation at temperatures up to 70°C higher than the ones of pure PLA. When silanes are present, thermal stability lowers as silane content increases, but it is anyway higher than the one of the pure polymer. © 2012 Wiley Periodicals, Inc. J. Appl. Polym. Sci. 000: 000–000, 2012

KEYWORDS: biopolymers and renewable polymers; nanostructured polymers; thermogravimetric analysis (TGA); differential scanning calorimetry (DSC)

Received 5 April 2012; accepted 22 August 2012; published online
DOI: 10.1002/app.38504

INTRODUCTION

Polylactic acid (PLA) is one of the most important commercially available, synthetic biodegradable polyester; however, brittleness[1] and low crystallization rate[2] limit its industrial applications. Low crystallization rate makes the polymer hardy suitable for injection molding processes and requires high production cycle times; on the other hand, brittleness does not allow for the production of engineering materials with good mechanical properties (i.e., low Izod–Charpy values). The use of nanofillers represents a good strategy to modify the physical and mechanical properties of PLA. In particular, nanoscale fillers can improve thermal stability of PLA and affect crystallization properties. Their effects on thermal behavior of PLA nanocomposites are described in literature, concerning the use of montmorillonite[3,4] or nanosilica[5] introduced both in compounding[6,7] or with *in situ* polymerization.[3,4]

In recent years, organic–inorganic nanocomposites with well-defined structures and morphology have become a very interesting and promising class of materials because of their potential use in a wide range of conventional application fields; particularly, among silica-based organic–inorganic nanocomposites,[8,9] PLA/nanosilica composites obtained via compounding have been already reported.[10–12] In these nanocomposites, silica can improve both thermal and mechanical properties. The advantages that can be obtained because of the mineral largely depend on the degree of mixing; as compatibility and adhesion between silica and PLA are rather poor, direct mixing of silica nanoparticles with PLA often leads to the aggregation of mineral particles and deterioration of mechanical properties. To overcome this drawback, it is necessary to modify the surface of silica particles to make them more compatible with the organic phase. The most common method is the modification of the silica particles with a surfactant or with silane-coupling agents; such modification, can greatly help to improve the thermal behavior and the mechanical properties and to reduce the brittleness, increasing melt viscosity and strength.[13–15]

In the first part of this work,[16] PLA/nanosilica composites were prepared by *in situ* polymerization of L-lactide using both standard silica nanoparticles and silica nanoparticles that were previously modified using different quantities of two commercially available silanes (an epoxy-terminated one and an

Applied Polymer SCIENCE

amino-terminated one). Organosilane modified nanosilicas are well dispersed in PLA, and the presence of surface modified nanoparticles contributes in increasing the viscosity of PLA nanocomposites without lowering the molecular weight.

In this article, the materials synthesized were further characterized, and the effects of fillers content and of the presence of silanes on thermal properties of PLA nanocomposites were investigated using differential scanning calorimetry (DSC) and thermogravimetric analysis (TGA).

EXPERIMENTAL

Materials and Methods

Synthetic methods have been described in detail in "Materials and Methods" section of the first article.[16] Pure PLA was synthesized in bulk using a 250 mL three-neck glass flask: 100 g of L-lactide were polymerized under nitrogen at 180°C for 2 h in the presence of tin octanoate (0.1% w/w) as catalyst, under mechanical stirring. L-lactide and tin octanoate were previously dried at 80°C under vacuum for 12 h. PLA/silica nanocomposites were synthesized using the same apparatus: L-lactide (100 g), nanosilica (0.5%–1.0%–2.0% w/w), and tin octanoate (0.1% w/w) were previously dried at 80°C under vacuum for 12 h.

DSC analyses were conducted using a Mettler Toledo DSC 820, on samples weighting from 7 to 10 mg each.

Dynamic DSC analyses samples were first heated from 25°C to 200°C at 10°C/min and maintained at 200°C for 2 min to eliminate residual internal stresses after the synthesis, then cooled down to −10°C at −50°C/min and maintained at −10°C for 2 min.

For T_m and T_c determination, samples were then first heated from 25°C to 200°C at 10°C/min, cooled from 200°C to 25°C at −10°C/min, and a second thermal cycle identical to the first one was then used to evaluate the behavior of the material. Figures 1–3 show only second heating cycle.

For crystallization kinetics determination, samples underwent six thermal cycles, heating at 20°C/min up to 200°C and then cooling down the sample to 25°C with different cooling rates: 10°C/min, 7.5°C/min, 5°C/min, 2°C/min, 1.5°C/min, and 1°C/min.

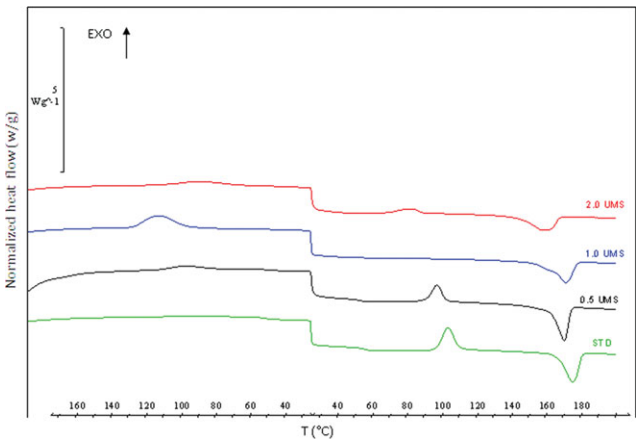

Figure 1. DSC curves of UMS samples compared with STD sample. [Color figure can be viewed in the online issue, which is available at wileyonlinelibrary.com.]

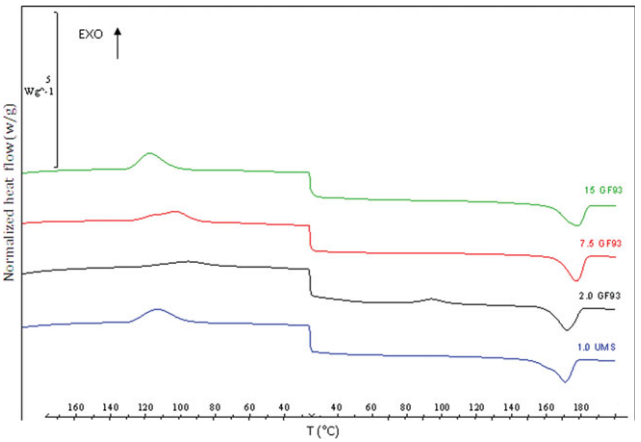

Figure 2. DSC curves of GF93 samples compared with 1.0 UMS sample. [Color figure can be viewed in the online issue, which is available at wileyonlinelibrary.com.]

Isothermal DSC analyses samples were heated to 200°C, kept at 200°C for 5 min, and then cooled at 100°C/min down to the temperature used for isothermal analysis. This temperature was maintained for 30 min to allow crystallization of the sample.

TGA analyses were conducted on a Perkin Elmer TGA4000 under nitrogen atmosphere on samples weighting 6 mg, heating from 50°C to 550°C (20°C/min).

RESULTS AND DISCUSSION

The synthesized samples are listed in Table I: STD is a standard linear PLA, UMS samples contain unmodified nanosilica, GF93 and GF80 samples contain silica modified with amino (GF93) and epoxy (GF80) silane.

DSC Analysis

In Figure 1, dynamic DSC curves of UMS samples show the effect of the presence of silica aggregates[16] on the formation of crystals, resulting in lower melting temperature and in a broadening of melting peak as silica content increases in comparison with standard PLA. This phenomenon is probably due to a

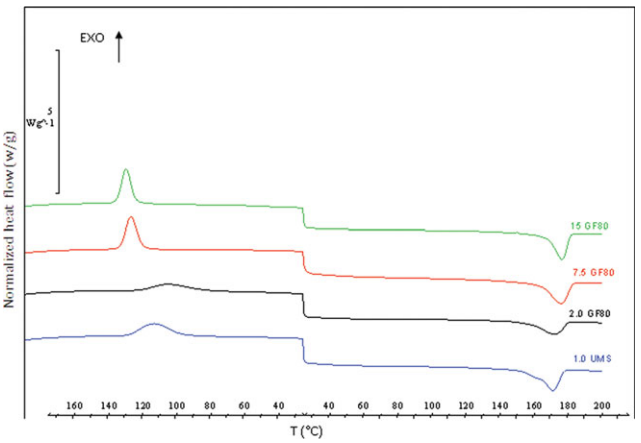

Figure 3. DSC curves of GF80 samples compared with 1.0 UMS sample. [Color figure can be viewed in the online issue, which is available at wileyonlinelibrary.com.]

Table I. Samples Synthesized

Sample	Silica (% w/w on lactide)	Silane	Silane added (% w/w on silica)
STD			
0.5 UMS	0.5		
1.0 UMS	1.0		
2.0 UMS	2.0		
2.0 GF93	1.0	Amino (GF93)	2
7.5 GF93	1.0	Amino (GF93)	7.5
15.0 GF93	1.0	Amino (GF93)	15
2.0 GF80	1.0	Epoxy (GF80)	2
7.5 GF80	1.0	Epoxy (GF80)	7.5
15.0 GF80	1.0	Epoxy (GF80)	15

different crystallization process caused by the presence of silica aggregates; similar phenomena have been already observed in literature.[17] Table II summarizes thermal data for STD PLA and nanocomposites samples; STD PLA sample shows a melting point (T_{m2}) of about 174°C and a melting enthalpy (ΔH_{m2}) of 53.90 J/g. The presence of silica nanoparticles lowers the melting point of the materials, but it leads to an increment of fusion heat, indicating an increase of crystallinity. This phenomena confirms that nanosilica acts as nucleating agent, and it increases the crystalline fraction, (χ),[18] that was evaluated using eq. (1)[17]

$$\chi = \frac{\Delta H}{\Delta H_m^0 * \left(1 - \frac{\%\text{wtfiller}}{100}\right)} * 100 \quad (1)$$

where χ is the crystalline fraction, ΔH is $\Delta H_{m2} - \Delta H_{c2}$ (related to second heating curves, as ΔH_{m2} is the specific melting enthalpy of the sample and ΔH_{c2} is the specific cold crystallization enthalpy of the sample), ΔH_m^0 is the melting enthalpy of the 100% crystalline polymeric matrix (93.0 J/g for PLA),[19] and %wt filler is the total weight percentage of silica.

Great differences can be observed in crystallization from the melt during cooling; STD PLA presents a broad and low crystallization peak with low crystallization enthalpy (ΔH_{c1}). In UMS samples, silica acts as heterogeneous nucleating agent; increasing its content from 0.5% to 1.0%, crystallization enthalpy increases (Table II) because the mineral acts as heterogeneous nucleating agent. When silica content was further increased up to 2.0%, crystallization temperature (T_{c1}) lowers, and also χ decreases probably because higher silica quantities perturb the reorganization of chains during cooling from the melt, as already observed in literature.[20,21]

Figure 1 also shows that T_g during second heating (T_{g2}) is lower or absent for UMS samples, and there is no significant change of this parameter caused by the addition of silica[7]; also cold crystallization during second heating (T_{c2} and ΔH_{c2}) is absent or lower when nanosilica is present.

Data show that 1.0 UMS is the sample with the highest crystallization temperature and melting enthalpy in comparison with STD sample; the effect of surface modification using silanes was therefore evaluated on samples containing 1% of nanosilica having different amounts of silane on the surface of the mineral.

A different behavior has been observed in DSC when silanes are present on the surface of nanosilica: as GF93 silane content increases, crystallization is easier and faster, resulting in an increase of crystallization enthalpy (ΔH_{c1}); also the amount of crystalline fraction increases as the quantity of silane increases.

However, 2.0 GF93 hardly crystallizes and a cold crystallization peak is observed during second heating indicating that crystallization was not complete (Figure 2).

A similar behavior has been observed for GF80 samples (Figure 3); these samples seem to show a higher affinity between polymeric matrix and silica, and this phenomenon results in higher crystallization rates and temperatures. The addition of high amounts of silane is responsible for increasing the crystalline fraction in comparison with 1.0 UMS sample due to an enhanced crystallization process, promoted by surface-modified nanosilica.

Nanocomposites containing surface modified nanosilica show higher melting temperature than 1.0 UMS sample.

Table II. DSC Analysis of Nanocomposites Samples in Comparison with STD Sample

Sample	T_{c1} (°C)	ΔH_{c1} (J/g)	T_{g2} (°C)	T_{c2} (°C)	ΔH_{c2} (J/g)	T_{m2} (°C)	ΔH_{m2} (J/g)	χ (%)	Onset (°C)	Endset (°C)	Δ (°C)
STD	96.9	5.2	55.0	102.8	46.1	174.1	53.9	8.4	113.5	60.7	52.8
0.5 UMS	97.8	20.0	52.3	96.4	31.8	169.0	54.3	24.3	115.3	76.9	38.4
1.0 UMS	113.5	56.7	-	-	-	170.2	56.0	60.8	128.7	96.6	32.1
2.0 UMS	90.2	29.0	-	81.8	13.5	157.6	50.0	40.0	114.2	61.9	52.3
2.0 GF93	96.2	35.0	-	93.8	16.3	171.3	56.9	44.1	122.1	75.0	47.1
7.5 GF93	103.3	52.0	-	-	-	176.5	58.0	62.9	127.9	89.7	38.2
15.0 GF93	118.2	57.6	-	-	-	176.9	60.0	65.2	129.4	103.0	26.4
2.0 GF80	105.6	41.9	-	-	-	170.9	42.0	45.6	122.7	80.7	42.0
7.5 GF80	127.6	57.5	-	-	-	175.0	57.8	62.7	133.3	120.4	12.9
15.0 GF80	130.3	62.0	-	-	-	175.5	62.0	67.3	135.4	124.6	10.8

Applied Polymer SCIENCE

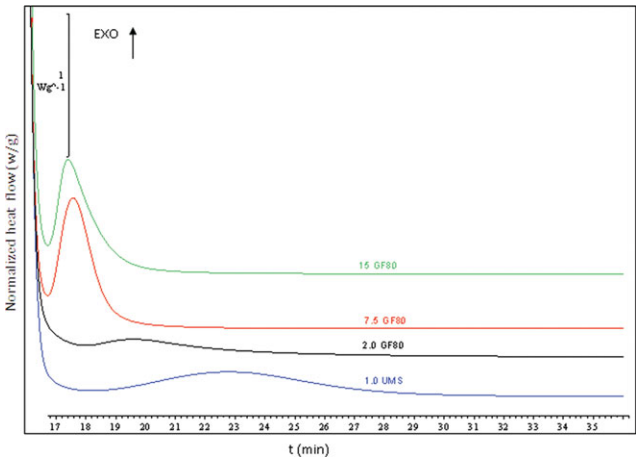

Figure 4. Isothermal crystallization curves of GF80 samples in comparison with 1.0 UMS, obtained at 137°C. [Color figure can be viewed in the online issue, which is available at wileyonlinelibrary.com.]

Also onset-endset temperatures (Table II) of crystallization peaks are useful to understand the different behavior of the samples; UMS samples do not have a linear behavior, as 1.0 UMS is by far the material having the lowest Δ and the highest onset temperature. Probably 0.5% of nanosilica is not enough to enhance the process and 2.0 % is too much, causing the formation of too many aggregates.[16]

When silanes are present, onset T of both 2.0 GF93 and 2.0 GF80 is lower than the one of 1.0 UMS and Δ is higher; this phenomenon is probably due to the presence on the surface of the mineral of a few long polymeric chains, having lower reorganization rates, together with many other chains.

Increasing silane content, onset temperatures increase and Δ lowers, especially for GF80 containing polymers; in these samples, there is a higher quantity of shorter chains on the surface of silica particles,[16,22] resulting in a more homogeneous system and in a faster reorganization. Epoxy silane reacts better during PLA polymerization and therefore gives the highest homogeneity, the highest onset temperature and the fastest crystallization.

Isothermal crystallization curves were used to further study the kinetic of the phenomenon; curves obtained at 137°C are shown in Figure 4, comparing polymers of the GF80 series and of the UMS series; surface modification increases both nucleation and rate of crystallization process.

Avrami Equation (2) has widely been used, also with PLA polymers[23] and with PLA/modified nanosilica added via melt blending,[24] and it may be considered to be valid for the studies on crystallization processes.

The reported equation was used to study the isothermal crystallization of the materials at different temperatures:

$$1 - X_c = e^{[-K_c t^n]} \tag{2}$$

or

$$\mathrm{Log}[-\ln(1 - X_c)] = n\,\mathrm{Log}\,t + \mathrm{Log}\,K_c$$

where X_c is the crystalline fraction, K_c is the kinetic crystallization constant, t is the time at which we observe the crystallization phenomenon, and n is Avrami number, dependent of the kind of crystallization phenomenon observed. The values of n and K_c determined are reported in Table III. Figure 5 presents plots of $\ln[-\ln(1 - X_t)]$ vs. $\ln(t)$ for the nanocomposites containing GF80 in comparison with 1.0 UMS sample at 137°C. Curves present a nonlinear behavior for higher times; in Figure 5 only, the data used to fit with Avrami equation are reported.

Avrami number, n, ranges from 1.2 to 2.4, and K_c tends to increase as the quantity of silane increases in comparison with UMS samples. GF80, the epoxy silane, gives higher K_c values; STD PLA has a very slow crystallization, and therefore n and K_c could not be measured in these analytical conditions.

GF80 samples show the highest K_c, while 1.0 UMS sample is the one having the lowest values; as silane content increases, there is a tendency to have faster crystallization kinetics, that for 15.0 GF80 sample are two magnitude orders greater than the ones of 1.0 UMS sample. This confirms the higher tendency to crystallization in samples having high quantities of silane, as they present faster crystallization kinetics and therefore enhance crystallization kinetics, besides increasing crystallization temperatures. The effect on Avrami number (n) is less marked but anyway 15.0 GF80 sample shows the lowest values among all samples and values are anyway lower for silane-containing samples. As already reported in literature,[24] it can be stated that n has no significant change; 15.0 GF80 samples, according to the theory

Table III. Avrami Parameters at Different Isothermal Crystallization Temperature

	136°C		137°C		138°C		140°C	
Sample	Log K_c	n	Log K_c	n	Log K_c	n	Log K_c	n
1.0 UMS	−1.55	2.1	−1.89	2.4	−1.89	1.7	−2.21	2.4
2.0 GF93	−1.99	1.6	−1.93	1.5	−1.78	1.4	−2.40	1.2
7.5 GF93	−1.51	1.7	−1.63	1.7	−1.68	1.6	−1.63	1.6
15.0 GF93	−1.39	2.0	−1.59	1.8	−0.88	1.8	−1.56	2.1
2.0 GF80	−1.50	1.9	−1.57	2.3	−1.61	1.5	−1.76	2.1
7.5 GF80	0.10	1.8	−0.02	1.5	−0.22	1.4	−0.70	1.3
15.0 GF 80	0.12	1.3	0.06	1.2	−0.17	1.2	−0.55	1.2

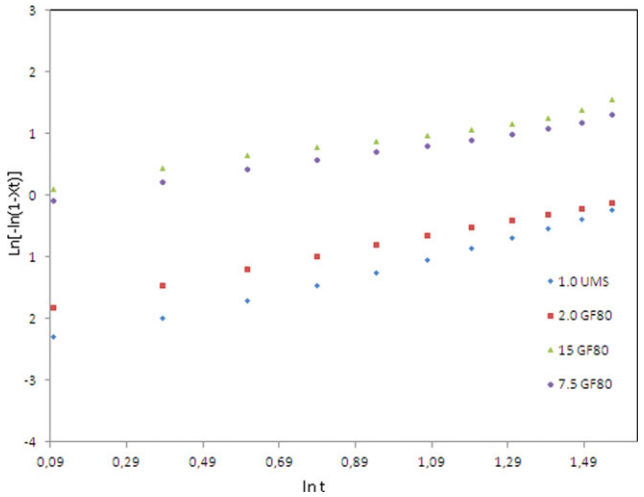

Figure 5. Plots of $\ln[-\ln(1 - X_t)]$ vs. $\ln(t)$ for GF80 nanocomposites and 1.0 UMS at 137°C. [Color figure can be viewed in the online issue, which is available at wileyonlinelibrary.com.]

related to the values of n seem to have an heterogeneous crystallization with a linear crystal growth ($n = 1$). On the other hand, for 15.0 GF93 sample, n is close to 2; this might indicate either a heterogeneous mechanism with a bi-dimensional crystal growth or a homogeneous mechanism with linear crystal growth. The differences in n values between the two silanes might be related to the different crystallization kinetics and heats observed in dynamic DSC experiments. 1.0 UMS sample has n close to 2; given its nature (no silane is present on the surface of nanosilica), this value probably indicates a heterogeneous crystallization with a bi-dimensional growth of the crystals.

Crystallization curves obtained with different cooling rates were performed to evaluate the behavior of the materials in quasi-isothermal conditions (slow cooling) or in nonequilibrium conditions (rapid cooling).

Temperatures of the crystallization peak at different cooling rates are reported in Table IV.

Table IV. Crystallization Peak Temperatures at Different Cooling Rates

Sample	T_{C10} (°C)	$T_{C7.5}$ (°C)	T_{C5} (°C)	T_{C2} (°C)	$T_{C1.5}$ (°C)	T_{C1} (°C)
STD	96.7	97.6	98.2	103.7	106.6	109.6
0.5 UMS	96.7	91.3	97.7	105.3	108.3	110.6
1.0 UMS	97.6	100.1	102.1	122.4	125.3	128.7
2.0 UMS	96.7	97.2	98.1	105.4	109.1	111.9
2.0 GF93	98.1	100.6	103.3	109.9	111.5	112.6
7.5 GF93	100.2	104.1	108.1	115.6	122.3	129.9
15.0 GF93	104.4	111.3	117.5	124.2	127.9	131.1
2.0 GF80	101.9	109.2	117.4	128.2	131.0	132.9
7.5 GF80	123.0	128.7	134.1	141.4	143.3	144.6
15.0 GF80	128.3	132.7	137.8	141.7	143.8	144.7

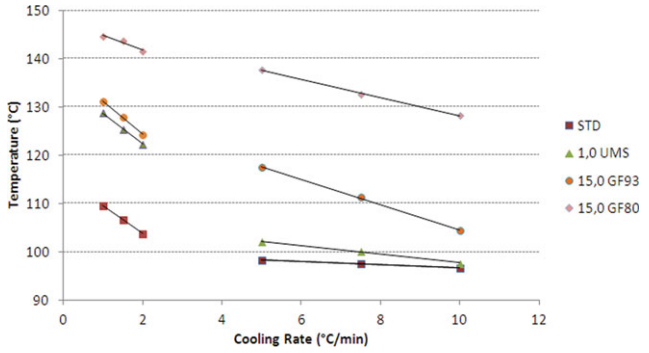

Figure 6. Crystallization peak temperature of some samples at different cooling rates. Samples containing surface treated silica always show higher crystallization peak temperatures. [Color figure can be viewed in the online issue, which is available at wileyonlinelibrary.com.]

Figure 6 reports some of the samples present in Table IV; there is a strong dependence of crystallization temperatures from cooling rate, as slow rates allow macromolecular chains to reorganize and to start nucleation processes earlier (at higher temperatures). 0.5 UMS and 2.0 UMS samples show results very similar to the ones of STD samples, but 1.0 UMS gives a marked increase of crystallization peak temperatures, especially with lower cooling rates; probably an intermediate quantity of nanosilica allows for a good dispersion of the mineral and gives enough heterogenic crystallization nuclei. When silane coupling agents are present, the effect of nanosilica is magnified, because of the improved dispersion of the mineral and the enhanced compatibility between inorganic and organic phases.

Crystallization enthalpy, especially at high cooling rates, cannot be determined with good accuracy; anyway, at lower rates, a higher crystallization heat is observed. GF80 samples present higher crystallization temperatures than GF93 samples and UMS samples, probably because of the higher reactivity of epoxy groups with the polymer in comparison with amino ones of GF93 silane. The different kinetics observed for all samples at low and high cooling rates may be related to the different growth of crystals. Low rates allow for longer reorganization times that allow the growth of well-formed crystals; on the other hand, when higher rates are used, a high number of small crystals are formed. This relation between cooling rate and dimension and shape of PLA crystals is known confirming that size of PLA spherulites increases when decreasing cooling rate.

TGA

Thermal data obtained with TGA are reported in Table V.

Thermal stabilities of PLA nanocomposites were evaluated from TGA thermograms checking temperature corresponding to 1%, 5%, 50%, and 95% of weight loss ($T_{1\%}$, $T_{5\%}$, $T_{50\%}$, and $T_{95\%}$).

Figure 7 shows TGA curves of UMS series; thermal stability increases markedly, especially increasing silica content; 2.0 UMS has a $T_{5\%}$ that is 70°C higher than the one of STD sample, reaching 346°C. On the other side, once degradation of 1.0 UMS and 2.0 UMS starts, it seems faster than degradation of STD, as $\Delta T_{1\%-95\%}$ goes from 104°C (STD sample) to 76°C for

Applied Polymer SCIENCE

Table V. Degradation Data of the Sample Synthesized

Sample	$T_{1\%}$ (°C)	$T_{5\%}$ (°C)	$T_{50\%}$ (°C)	$T_{95\%}$ (°C)	$\Delta T_{1\%-95\%}$ (°C)
STD	248	275	320	352	104
0.5 UMS	270	305	354	382	113
1.0 UMS	313	335	372	389	76
2.0 UMS	297	346	381	392	95
2.0 GF93	273	314	357	375	102
7.5 GF93	254	284	334	372	118
15.0 GF93	253	278	325	376	123
2.0 GF80	286	315	364	390	104
7.5 GF80	275	301	350	383	108
15.0 GF80	264	280	326	381	117

1.0 UMS sample. Only sample 0.5 UMS has a degradation kinetic similar to the one of STD; the increase in thermal stability is correlated with the formation of a network between PLA and nanosilica.[16] The rise of stability of PLA containing unmodified nanosilica in TGA was already observed in the literature[25] on samples obtained via compounding using Natureworks 4032D PLA as polymeric matrix; the phenomenon occurs because the network reduces the mobility of PLA chains and the activity of terminal hydroxyl groups responsible for the decomposition reactions. In our samples, obtained via *in situ* polymerization, the increase of stability in comparison with pure PLA is much higher than the same amount of nanosilica. The higher degradation onset of pure PLA observed in the article by Dong and coworkers[25] is owed to the presence of stabilizers in the commercial polymer.

Figures 8 and 9 show TGA curves of GF93 and GF80 samples. $T_{5\%}$ and $T_{50\%}$ lower increasing silane content but are higher than the ones of STD anyway; 15.0 GF93 has a $T_{5\%}$ of 278°C, slightly higher than the value for STD sample. The lowering of degradation temperature in comparison with UMS samples, especially increasing silane content, can be explained considering that silanes have the tendency to degrade at relatively low temperatures forcing the beginning of the degradation process of the nanocomposite material. Moreover, a higher quantity of silanes creates a higher number of terminal groups, able to

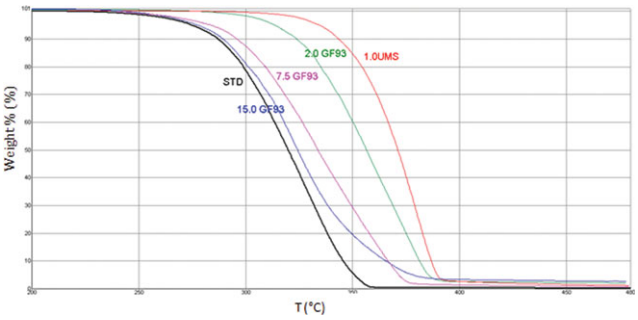

Figure 8. TGA curves of GF93 samples compared with STD one. [Color figure can be viewed in the online issue, which is available at wileyonlinelibrary.com.]

enhance a faster thermal degradation, as they are less stable than the internal groups of the macromolecular chains. Nanocomposites of the GF80 series have $T_{5\%}$ and $T_{50\%}$ temperatures slightly higher than the ones of GF93 samples, but data are very similar. Table V evidences that both GF93 and GF80 samples have a $\Delta T_{1\%-95\%}$ that increases when silane content increases and that becomes higher than the one of STD sample; silanes force the beginning of the degradation process, but once silane is completely degraded, the system behaves similarly to UMS samples; this hypothesis is confirmed by $T_{95\%}$ temperatures that are very similar for all silica-containing systems.

CONCLUSIONS

Thermal properties of PLA/silica nanocomposites were evaluated by DSC and TGA; silica was used both as such and after surface modification with different amounts of two silanes, an amino derivative and an epoxy containing compound.

DSC scans show that T_m becomes lower when nanosilica is present, especially at high loadings (2% w/w) but, once higher quantities of silanes are used, T_m becomes even slightly higher than the ones of standard polymer, probably due to the improved compatibility between the organic matrix and silica.

Higher crystallinity and faster crystallization kinetic were observed in presence of silica and especially with properly silanes-modified silica. Isothermal crystallization kinetic (evaluated using Avrami equation) becomes much faster, giving

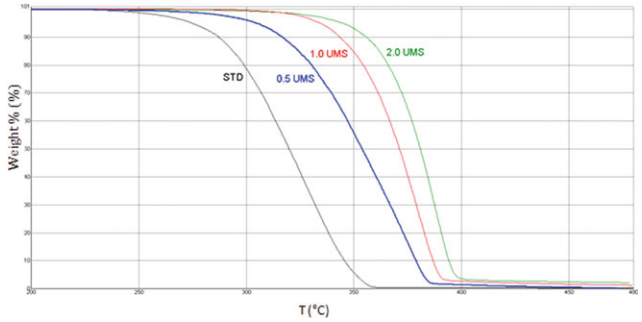

Figure 7. TGA curves of UMS samples compared with STD one. [Color figure can be viewed in the online issue, which is available at wileyonlinelibrary.com.]

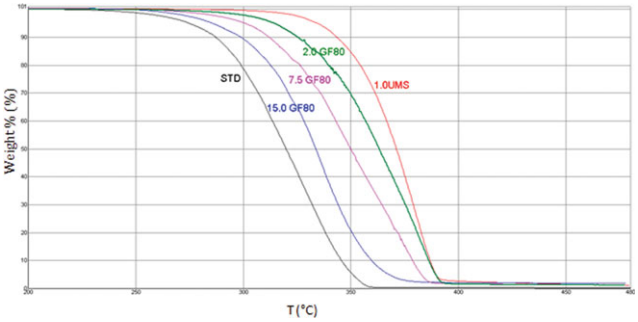

Figure 9. TGA curves of GF80 samples compared with STD one. [Color figure can be viewed in the online issue, which is available at wileyonlinelibrary.com.]

values of K_c that are two magnitude orders greater than the ones of the sample with unmodified silica. The presence of many short polymeric chains growing from silica surface is probably responsible for the improved nucleating effect of silica when silanes are present and, in turn, of the faster kinetic to an enhanced crystallization process can allow for polymers more suitable for injection molding and having improved mechanical properties in the material.

TGA data show that unmodified silica markedly increases degradation temperatures; when silanes are present on the surface of silica, degradation temperature becomes similar to the ones of standard PLA but the process seems slower, having a $\Delta T_{1\%-95\%}$ higher than the one of standard sample and much higher than the one of samples containing unmodified silica. $\Delta T_{1\%-95\%}$ increases as silane content becomes higher. Samples have therefore enhanced thermal stability in comparison with standard PLA, making them less sensitive to processing.

ACKNOWLEDGMENTS

This work has been performed on thanks to the financial support of *Fondazione Cariplo*, for the project "Nanocomposite PLA with complex macromolecular architecture for high performances in packaging."

REFERENCES

1. Ikada, Y.; Tsuji, H. *Macromol. Rapid Commun.* **2000,** *21*, 117.
2. Tsuji, H. In Recent Research Developments in Polymer Science; Pandalai, S. G., Ed.; Transworld Research Network: Trivandrum, India, **2000; Vol.** *4*, p 13.
3. Paul, M. A.; Alexandre, M.; Degée, P.; Calberg, C.; Jérôme, R.; Dubois, P. *Macromol. Rapid Commun.* **2003,** *24*, 561.
4. Paul, M. A.; Delcourt, C.; Alexandre, M.; Degée, P.; Monteverde, F.; Rulmont, A.; Dubois, P. *Macromol. Chem. Phys.* **2005,** *206*, 484.
5. Fukushima, K.; Tabuani, D.; Abbate, C.; Arena, M.; Rizzarelli, P. *Eur. Polym. J.* **2011,** *47*, 139.
6. Il-Hwan, K.; Young Gyu, J. *J. Polym. Sci. Part B: Polym. Phys.* **2010,** *48*, 850.
7. Chow, W. S.; Lok, S. K. *J. Therm. Anal. Calorim.* **2009,** *95*, 627.
8. Kasiwagi, T.; Morgan, A. B.; Antonucci, J. M.; Van Landingham, M. R.; Harris, R. H., Jr.; Awad, W. H.; Shields, J. R. *J. Appl. Polym. Sci.* **2003,** *89*, 2072.
9. Peng, Z.; Kong, L. X.; Li, S. D.; Chen, Y.; Huang, M. F. *Compos. Sci. Technol.* **2007,** *67*, 3130.
10. Huang, J. W.; Yung, C. H.; Ya-Lan, W.; Chiun-Chia, K.; Mou-Yung, Y. *J. Appl. Polym. Sci.* **2009,** *112*, 1688.
11. Huang, J. W.; Yung, C. H.; Ya-Lan, W.; Chiun-Chia, K.; Mou-Yung, Y. *J. Appl. Polym. Sci.* **2009,** *112*, 3149.
12. Wen, X.; Lin, Y.; Han, C.; Zhang, K.; Ran, X.; Li, Y.; Dong, L. *J. Appl. Polym. Sci.* **2009,** *114*, 3379.
13. Yan, S. F.; Yin, J. B.; Yang, Y.; Dai, Z. Z.; Ma, J.; Chen, X. S. *Polymer* **2007,** *48*, 1688.
14. Zhu, A.; Diao, H.; Rong, Q.; Cai, A. *J. Appl. Polym. Sci.* **2010,** *116*, 2866.
15. Wu, D.; Wu, L.; Wu, L.; Zhang, M. *Polym. Degrad. Stab.* **2006,** *91*, 3149.
16. Basilissi, L.; Di Silvestro, G.; Farina, H.; Ortenzi, M. A. *J. Appl. Polym. Sci.*, in press; DOI: 10.1002/APP.38324.
17. Battegazzore, D.; Bocchini, S.; Frache, A. *Express Polym. Lett.* **2011,** *5*, 849.
18. Kontou, E.; Niaounakis, M.; Georgiopoulos, P. *J. Appl. Polym. Sci.* **2011,** *122*, 1519.
19. Turner, J. F.; Riga, A.; O'Connor, A.; Zhang, J.; Collis, J. *J. Therm. Anal. Calorim.* **2004,** *75*, 257.
20. Papageorgiou, G. Z.; Achilias, D. S.; Nanaki, S.; Beslikas, T.; Bikiaris, D. *Thermochim. Acta* **2010,** *511*, 129.
21. Tjong, S. C.; Bao, S. P. *J. Polym. Sci. Part B: Polym. Phys.* **2004,** *42*, 2878.
22. Joubert, M.; Delaite, C.; Bourgeat-Lami, E.; Dumas, P. *J. Polym. Sci. Part A: Polym. Chem.* **2004,** *42*, 1976.
23. Miyata, T.; Masuko, T. *Polymer* **1998,** *39*, 5515.
24. Yougang, G.; Yudong, Z.; Xiangmin, X.; Puyu, Z. *Zhongguo Suliao* **2010,** *24*, 30.
25. Wen, X.; Zhang, K.; Wang, Y.; Han, L.; Han, C.; Zhang, H.; Chen, S.; Dong, L. *Polym. Int.* **2011,** *60*, 202.